GEOPHYSICAL RESEARCH LETTER, VOL. 20, NO. 1, PAGES 41-44, JANUARY 8, 1993

ARCTIC SEA ICE ALBEDO: A COMPARISON OF TWO SATELLITE-DERIVED DATA SETS

Axel J. Schweiger, Mark C. Serreze and Jeffrey R. Key

Cooperative Institute for Research in Environmental Sciences
Division of Cryospheric and Polar Processes
University of Colorado, Boulder

Abstract. Spatial patterns of mean monthly surface albedo for May, June, and July, derived from DMSP Operational Line Scan (OLS) satellite imagery are compared with surface albedos derived from the International Satellite Cloud Climatology Program (ISCCP) monthly data set. Spatial patterns obtained by the two techniques are in general agreement, especially for June and July. Nevertheless, systematic differences in albedo of 0.05 - 0.10 are noted which are most likely related to uncertainties in the simple parameterizations used in the DMSP analyses, problems in the ISCCP cloud-clearing algorithm and other modeling simplifications. However, with respect to the eventual goal of developing a reliable automated retrieval algorithm for compiling a long-term albedo data base, these initial comparisons are very encouraging.

1. Introduction

Variations in the surface albedo of the Arctic pack ice cover is an important factor in the long-term mass balance and stability of the pack ice. Continued monitoring of albedo is consequently an important component of the "early detection" strategy for identifying global and regional climate changes. Nevertheless, until recently, studies of the Arctic Ocean albedo have been of limited spatial and temporal scope, based largely on observations at drifting stations, fast ice, and during aircraft missions. Other investigators have used these measurements and satellite passive microwave data to estimate regional summer albedos [see *Robinson et al.*, 1992 and references therein].

With the aim of developing a long-term record *Robinson et al.* [1992] recently developed a ten year data set of parameterized albedo for the entire Arctic Ocean for May through mid-August. Maps of surface brightness charted through manual analysis of visible-band DMSP imagery were converted to parameterized surface albedo. Although lacking radiometric control, this data base (hereafter referred to as the RO92 set) has allowed for definition of the climatological characteristics of albedo. More recently, we have compiled a separate albedo data set, based on AVHRR channel 1 (0.6 μm) reflectances from the International Satellite Cloud Climatology Program (ISCCP) monthly (C2) data set in conjunction with modeled snow spectral reflectances. Here, we compare these two data sets for the months of May, June, and July. While providing an evaluation of uncertainties in our current knowledge of Arctic Ocean surface albedo, this paper also addresses problems in the automated extraction of these data, and clarifies aspects of the existing retrieval algorithm in need of further attention.

Paper number 92GL03006
0094-8534/93/92GL-03006$03.00

2. Data and Methods

2.1. *ISCCP Albedos*

The ISCCP-C2 data set [*Rossow and Schiffer*, 1991] contains cloud amount, cloud optical depth, 0.6 μm surface reflectivity, surface temperature, as well as atmospheric profiles of temperature, water vapor and ozone. These parameters are derived almost exclusively from satellite. By design the ISCCP data set is suitable for calculation of radiative fluxes at the surface and the top of the atmosphere. While the ISCCP data set constitutes an ongoing effort starting in July 1983, only data through 1986 were available at the time of this analysis. Additionally, we restrict our study to ocean areas north of 62.5° latitude.

The spectrally integrated albedo of a snow or ice-covered surface depends not only on the spectral albedo of the surface but also on the spectral distribution of the downwelling shortwave radiation. Since the ISCCP data set only reports reflectivities at 0.6 μm, radiative transfer calculations were performed to obtain spectrally integrated albedos comparable to the RO92 set. Here we use the radiative transfer model of *Tsay et al.* [1989]. Gas absorption is parameterized for 24 spectral bands. Atmospheric temperatures reported in the ISCCP data set were supplemented with inversion statistics from drifting ice islands. Approximately 10 vertical layers are used. Clouds are modeled as Mie scattering layers of variable thickness, with physical top height and optical thickness given in the ISCCP data set. Cloud physical thickness is calculated assuming an effective radius and liquid water concentration consistent with the ISCCP retrieval algorithm. Since the ISCCP data set only provides a single channel (0.6 μm) measurement of surface reflectivity, reflectivities for the remaining spectral bands in the radiative transfer scheme have to be inferred from this measurement based on the surface types. The surface is assumed to be a mixture of no more than three types, selected depending on season from a catalog consisting of fresh snow, old melting snow, melt ponds, bare ice, and open water. For example, in

Table 1. DMSP-based albedo classes.

Class	Clear-sky Albedo	Standard Deviation	All-sky Albedo
1	0.75	0.04	0.80
2	0.59	0.07	0.64
3	0.44	0.08	0.49
4	0.27	0.05	0.29

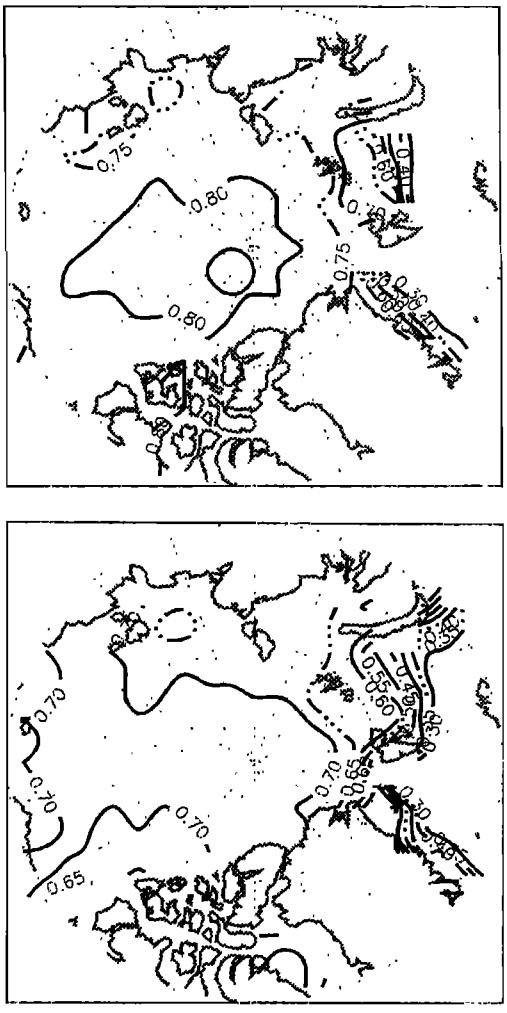

Fig. 1. Mean monthly albedo for May from the RO92 (top) and the ISCCP C2 (bottom) data sets.

June when the snow cover is melting the prescribed surface types are ice, melt ponds and open water. Given the 0.6 μm reflectivity for the entire cell, the ice concentration contained in the ISCCP data set (from the Navy/NOAA Joint Ice Center (JIC) charts), and expected 0.6 μm reflectivities for each of the assumed surface types, the fractional area of melt ponds can be calculated. If the calculated melt pond coverage is unrealistic (e.g., if it is present when only snow and open water are assumed to exist or when the coverage is greater than 50%), 0.6 μm snow reflectivities are adjusted to match observed values.

Reflectivities for the 24 shortwave bands (total range of 0.28-4.0 μm) were computed for the two snow types assuming Mie scattering of ice grains and soot particles [*Warren and Wiscombe*, 1980]. Spectral reflectivities of melt ponds and bare ice were taken from *Grenfell and Maykut* [1977], with open water reflectivities computed after *Brieglieb et al.* [1986]. Snow reflectivities in the remaining 23 bands are determined assuming constant ratios to 0.6 μm reflectivities. The fractional coverage of each surface type is then used to calculate the integrated surface reflectivity over all 24 bands. Monthly albedos are calculated as the ratio of the upwelling and downwelling shortwave fluxes computed by the model for both clear and cloudy conditions.

2.2. *DMSP Data Set*

The RO92 data set is based on a manual charting of surface brightness changes in three-day increments over the entire Arctic Ocean for May-mid August of 1975, 1977-1980 and 1984-1988. Analyses are based primarily on 2.7 km resolution DMSP OLS orbital swath images. These data, which provide daily Arctic-wide coverage, are archived as transparencies only, produced operationally from digital data in a broad-band channel spanning the visible and near-infrared (0.4-1.1 μm) wavelengths. DMSP images with local coverage at a 0.6 km resolution and NOAA Advanced Very High Resolution Radiometer (AVHRR) 1.1 km resolution visible-band images, were used only when the 2.7 km DMSP products were missing from the archive or of poor quality [see *Scharfen et al.*, 1987 and *Robinson et al.*, 1992 for details]. Extensive cloud cover and poor lighting precluded charting after mid-August. Since the ISCCP-based albedos are monthly means, and albedo can change very rapidly during August, we eliminate this month from the analysis.

Efforts were made to chart the brightness of what appears on the images as snow/ice, ignoring the effects of large leads and polynyas. However, no adjustments are made for undetected open water areas. Four brightness classes were defined [*Scharfen et al.*, 1987; *Robinson et al.*, 1992]. Available surface and aircraft observations indicate that brightness class 1 corresponds to fresh snow cover over 95% of the ice; class 2 is found when snow covers between 50-95% of the surface, with the remainder being bare or ponded ice; class 3 represents the advanced to final stage of snow melt with numerous melt ponds and between 10-50% of the ice surface snow covered, or, following pond drainage, predominantly bare ice; class 4 is heavily-ponded or flooded ice.

The surface brightness maps were digitized to the Limited-Area Fine Mesh version of the U.S. National Meteorological Center grid, dividing the Arctic Ocean into 223 cells. Grid cells were simply assigned the value of the predominant brightness class in that cell, with open-water cells defined using JIC ice concentration charts closest in time to the analyzed three-day interval, digitized to the same grid. Cells with missing data (e.g., cloud cover) were assigned the values of corresponding cells from the immediately preceding chart or subsequent chart if available. Data were usually available over more than 90% of all cells for each chart.

Parameterized albedos were next assigned to each grid cell. Digital numbers (DNs) were measured for sea ice and open water within rectangular regions of approximately 9000 km^2 from clear-sky portions of 20 digitized DMSP transparencies for May through July of 1977 and 1979. Both the 0.6 km and 2.7 km DMSP products were used. The highest mean DN values of snow-covered sea ice and the lowest mean DN of open water were then used as tie points and assigned clear-sky albedos based on measured ground and aerial data. The upper tie-point brightness was assigned an albedo of 0.79 until late June, after which a value of 0.69 was used, due to the decrease in maximum image brightness associated with snow melt [*Robinson et al.*, 1992]. The albedo of open water cells was taken as 0.12 [*Cogley*, 1979]. The literature values of albedo, and hence our resultant values, refer to the integrated solar spectral range of approximately 0.3-2.7 μm.

The average DNs from regions corresponding to the

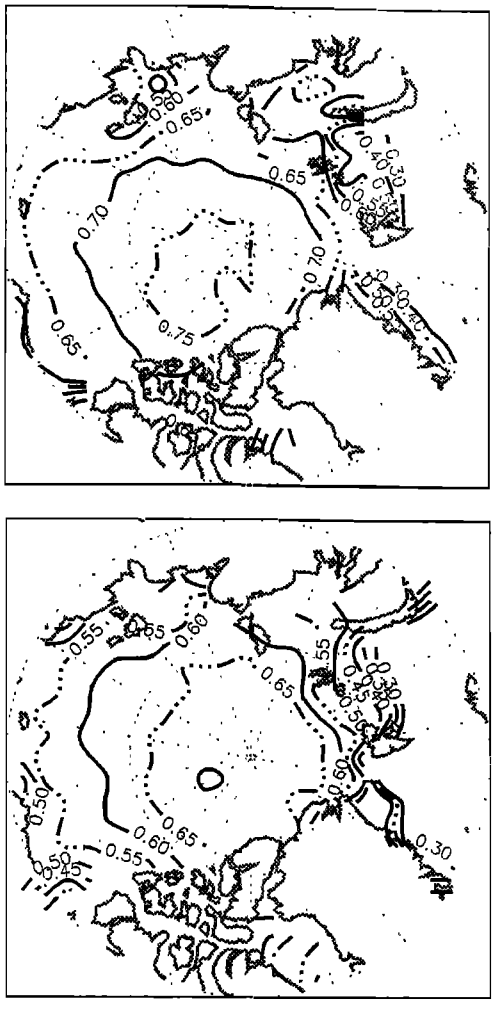

Fig. 2. Same as Figure 1, but for June.

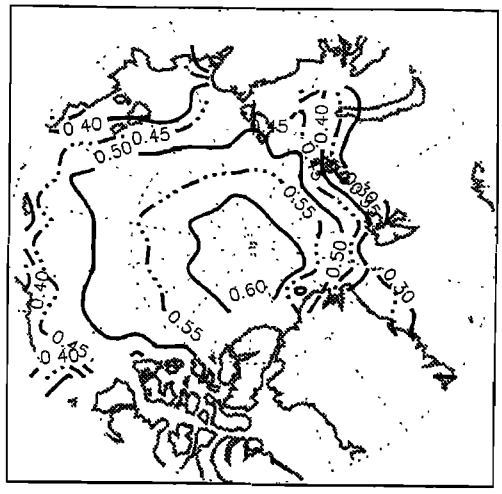

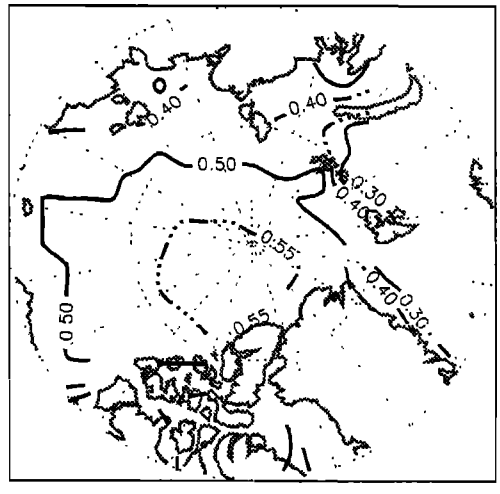

Fig. 3. Same as Figure 1, but for July.

charted classes were then converted into clear-sky albedos by linear interpolation between the tie points. Mean values and their standard deviations are given in Table 1. Cloud cover tends to increase albedo due to preferential absorption of near-infrared radiation where snow reflectance is low relative to visible wavelengths. To obtain albedo values representative of typical Arctic cloud cover conditions, the clear-sky albedos were increased by 0.05 for brightness classes 1-3 and 0.02 for class 4, based on published data [see *Robinson et al.*, 1992].

3. Results

Figures 1 through 3 show the spatial patterns of mean monthly surface albedo from the RO92 and ISCCP data sets for May through July. During May, when snow melt is largely confined to coastal regions [*Robinson et al.*, 1992] both data sets show little spatial variability over the central Arctic. The RO92 albedos over the central Arctic tend to be between 0.75 and 0.80 (the latter figure representing the maximum possible parameterized value). By contrast, the ISCCP values over the same regions are lower by about 0.05 to 0.10. Both data sets show a strong gradient of decreasing albedo near coastal regions, especially toward the Norwegian and East Siberian Seas, consistent with the effects of decreasing ice concentrations and coastal snow melt [*Robinson et al.*, 1992]. Both data sets also show surface albedos to be lower near the New Siberian Islands. The reduction in albedo near the western portion of the Canadian Arctic Archipelago shown by ISCCP, however, is not depicted in the RO92 analysis.

By June, melt is underway over large areas of the sea ice cover [*Robinson et al.*, 1992] which results in a decrease in surface albedo (Figure 2). Both data sets show a concentric pattern of surface albedos, with values decreasing from the pole southwards. *Serreze et al.* [1991] show that this concentric pattern can be related to the climatological distribution of melting degree days. ISCCP albedos, however, again tend to be lower than those reported by RO92. For example, in the central Arctic regions ISCCP tends to be lower by about 0.1.

Albedos continue to decline during July (Figure 3). The concentric pattern observed in both data sets for June is still present. During July the ISCCP and RO92 albedos match very well, except near the pole where ISCCP albedos are now higher than the RO92 values by up to 0.05.

4. Discussion

The RO92 and ISCCP data sets are in good agreement with respect to spatial patterns, especially for June and July. These spatial patterns also compare favorably with the summary of surface melt prepared by *Marshunova and*

Chernigovskiy [1978], in which a concentric pattern of melt over the Arctic pack ice progressing towards the pole by early July is evident. However, there are systematic differences in the absolute values reported of the two data sets examined here, on the order of 0.10. Specifically, the ISCCP albedos during May and June are lower than the RO92 values, but are larger during July near the Pole. There is probably no single reason for these discrepancies.

Regarding likely candidates, it may be significant that the present ISCCP algorithm assumes that clouds have a higher channel 1 reflectivity than the surface. In the polar regions this is not always the case. Thus, surfaces displaying higher AVHRR channel 1 reflectivities are excluded from the clear sky composite, biasing the ISCCP results towards lower surface albedos. On the same basis, the ISCCP algorithm appears to underestimate cloud amounts in the Arctic [*Schweiger and Key*, 1992] and since the spectrally integrated albedo of snow-covered surfaces under cloudy conditions can exceed clear sky values by more than 0.1, an underestimate of total cloud amount may also explain why ISCCP albedos are too low. Furthermore, in the calculation of spectrally integrated albedos from the ISCCP data set, a number of assumptions are made regarding the spectral albedos and distribution of surface types; e.g., grain size and soot content of the snow. Since the ratio of visible band to near infrared reflectivity of snow is chiefly determined by those factors, spectrally integrated albedos for clear sky conditions are rather sensitive to their specification. Furthermore, the ISCCP retrieval algorithm neglects the optical effects of aerosols which, particularly in the Arctic, can significantly effect the clear sky composite.

Regarding the RO92 analyses, one may argue that a human interpreter should provide a more accurate cloud/snow discrimination. This data does contain an adjustment of albedo by climatological cloud amounts but, given its crudity, this may further contribute to the differences between the two data sets. More generally, the fundamental limitation of the RO92 set is that it lacks radiometric control. Only four albedo classes are provided, each with a large standard deviation. Angular and atmospheric effects are ignored, as are the effects of nonlinearities in the original photographic recording process.

Finally, one must also consider that since the ISCCP data are for four years only (1983-1986), compared to the 10-year RO92 data set, part of the problem may also lie in the natural interannual variability of albedo. The RO92 data set is not considered appropriate for addressing interannual variability [*Robinson et al.*, 1992], especially with respect to the use of only four class albedos. As such, we leave this point as an open issue.

5. Conclusions

Generally good agreement in the spatial patterns of surface albedo is found between RO92 and ISCCP data sets. While the RO92 data set cannot be considered "ground truth", the similarity between albedo patterns in these two independently-derived products gives a positive outlook for operational retrieval of albedo from satellite data. However, there are systematic differences in the absolute albedo values, with ISCCP albedos being lower during May-June and higher in July. Reasons for these differences presumably reflect the present inadequacies in the ISCCP cloud-clearing algorithm and the simplifications and subjectivity in the RO92 procedures. Because of these uncertainties it is not currently possible to determine which is more correct. It may be that the true albedos lie somewhere between those of the two analyses.

Acknowledgements. This study was supported by NSF Grant ATM 90-16563 and NASA grants NAGW-2158 and NAGW-2407 (University of Washington subcontract 721566).

References

Brieglieb, B.P, P. Minnis, V. Ramanathan and E. Harrison, Comparison of Regional Clear-Sky Albedos Inferred from Satellite Observations and Model Computations. *J. Clim. Appl. Meteor.*, 25, 214-226, 1986.

Cogley, J.G., The albedo of water as a function of latitude. *Mon. Wea. Rev.*, 107, 775-781, 1979.

Grenfell, T.C, and G.A. Maykut, The optical properties of ice and snow in the Arctic basin. *J. Glaciol.*, 18(80), 445-463, 1977.

Marshunova, M.S., and N.T. Chernigovskiy, *Radiation Regime of the Foreign Arctic.* Gidrometeoizdat, Leningrad, Nat. Sci. Found. Tech. Translation 72-51034, 1978.

Robinson, D.A, M.C. Serreze, R.G. Barry, G. Scharfen, and G. Kukla, Large-scale patterns and variability of snow melt and parameterized surface albedo in the Arctic Basin, *J. Climate*, 5(10), 1109-1119, 1992.

Rossow, W.B., and R.A. Schiffer, ISCCP Cloud Data Products. *Bull. Amer. Meteorol. Soc.* 72(1), 2-20, 1991.

Schweiger, J.A and J. Key, Arctic Cloudiness: Comparison of ISCCP-C2 and Nimbus-7 Satellite-Derived Cloud Products with a Surface-Based Cloud Climatology. *J. Climate*, 5(12), 1514-1527, 1992.

Scharfen, G., R.G. Barry, D.A. Robinson, G. Kukla and M.C. Serreze, Large-scale patterns of snow melt on arctic sea ice mapped from meteorological satellite imagery. *Ann. Glaciol.*, 9, 1-6, 1987.

Serreze, M.C., T.L. Dermaria, R.G. Barry and D.A. Robinson, *Atmospheric forcings on large-scale patterns of parameterized albedo over Arctic sea ice: case studies for June 1975 and 1988*, Proceedings, Fifth Conference of Climate Variations, October 14-18, Denver, CO, Am. Meteor. Soc., 396-399, 1991.

Tsay, Si-Chee, K. Stamnes and K. Jayaweera, Radiative Energy Budget in the Cloudy and Hazy Arctic, *J. Atmos. Sci.*, 46(7), 1002-1018, 1989.

Warren, S.G., and W.J. Wiscombe, A model for the spectral albedo of snow II. Snow containing atmospheric aerosols. *J. Atmos. Sci.*, 37, 2734-2745, 1980.

A.J. Schweiger, M.C. Serreze and J.R. Key, Cooperative Institute for Research in Environmnetal Sciences, Division of Cryospheric and Polar Processes, University of Coloardo, Boulder, CO 80309-0449

(Received July 20, 1992;
accepted November 6, 1992.)